

a_p -index solar wind driving function and its semiannual variations

A. A. Petrukovich and M. Y. Zakharov

Space Research Institute, 84/32 Profsoyuznaya st., Moscow, 117997, Russia

Received: 17 April 2007 – Revised: 18 June 2007 – Accepted: 27 June 2007 – Published: 30 July 2007

Abstract. Semiannual variation of geomagnetic activity and a_p -index in particular is supposed to consist of heliospheric factor (axial hypothesis and Russell-McPherron effect) and magnetospheric/ionospheric factor (equinoctial hypothesis). In our investigation we express a_p -index as a magnetospheric response function to solar wind and IMF input. Seasonal variation in a_p -index on average (1963–2003) is ~ 4 nT and consists of ~ 2.1 – 2.3 nT of magnetospheric/ionospheric part, 0.6–1.3 nT of heliospheric part (including 0.2–0.3 nT of R-M effect), 0.1–0.4 nT is due to the non-linear term. 90% confidence range of all estimates is ~ 0.1 – 0.25 nT. While autumn/spring magnetospheric response functions are almost identical, there is substantial difference between winter and summer functions. The increase of solar wind input in autumn and spring is also different by a factor of two.

Keywords. Magnetospheric physics (Solar wind-magnetosphere interactions)

1 Introduction

Semiannual variation (SAV) of geomagnetic activity with maxima near equinoxes appears in several forms, such as a periodic wave in geomagnetic indices like a_p (Russell and McPherron, 1973; Svalgaard, 1977; Cliver et al., 2000; Le Mouel et al., 2004), or a tendency of strong storms to occur during spring/autumn (Cliver et al., 2004; Svalgaard et al., 2002). In-depth reviews of previous publications can be found elsewhere (Cliver et al., 2000; Russell and McPherron, 1973).

Generally three different sources of SAV are suggested: (1) Equinoctial hypothesis relates SAV with the angle between geomagnetic dipole and solar wind flow, controlling

basically sensitivity of the magnetosphere (McIntosh, 1959). However specific physical mechanism is still not identified, and, e.g., solar illumination of ionosphere is suggested as alternative (Lyatsky et al., 2001). (2) Cortie effect or axial hypothesis (Cortie, 1912; Bohlin, 1977) attributes SAV to increase of heliographic latitude around equinoxes, placing Earth closer to more geoefficient fast solar wind streams from mid-latitude coronal holes. (3) Russell-McPherron (RM) effect points that spiral IMF B_y in GSEQ frame contributes to geoeffective IMF B_z in GSM (Russell and McPherron, 1973). Essentially sources (2) and (3) are solar wind effects external to the magnetosphere.

Here we concentrate on SAV in A -family indices (Fig. 1). With a recent investigation of SAV phases it was shown that 65–75% of this variation is due to equinoctial effect, axial effect contributes of the order of 20%, while the RM effect is the smallest with $\sim 10\%$ (Cliver et al., 2000, 2002). The RM and axial effects depend on actual distribution of, e.g., IMF polarity sectors in particular dataset, and their contribution may vary from year to year (Cliver et al., 2004).

However consistent analysis of SAV, representing an index as an explicit function of solar wind input and magnetospheric response was not performed. This is the main task of our investigation.

2 The solar wind input model

Our investigation is based on 3-h a_p index and OMNI-2 solar wind data for the period 1963–2003. Only 57 403 samples with available simultaneous solar wind and IMF measurements were considered (the total number is 109 800).

A standard approach to solar wind geoeffectiveness is to approximate an index with a combination of solar wind and IMF characteristics (driving function). $V B_s$ is the simplest driving function. Among other suggested expressions are $V^2 B_s$ and epsilon-parameter $\epsilon \sim V B^2 \sin^4 \theta / 2$. Moderate

Correspondence to: A. A. Petrukovich
(apetruko@iki.rssi.ru)

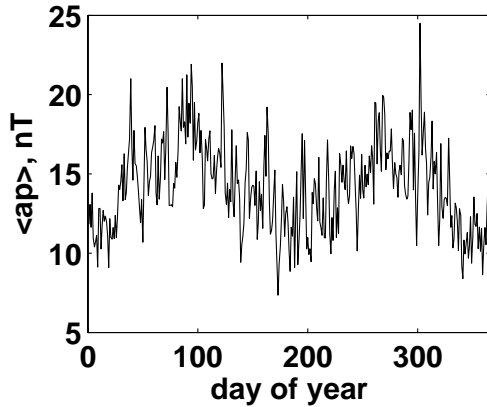


Fig. 1. Seasonal periodicity in daily a_p index averages.

solar wind density or dynamic pressure effect is sometimes considered as, e.g., $\sim(NV^2)^{-1/3}$ (review of Gonzalez et al., 1994). Here $B_s = -B_z$ for $B_z < 0$ and $B_s = 0$ for $B_z > 0$, B is IMF in GSM frame of reference, V , N – solar wind speed and number density. θ is the IMF clock angle, $\tan(\theta) = B_y/B_z$. Optimal functions might be different for different indices and time scales (Petrukovich, 2006; Finch and Lockwood, 2007).

The driving function, suitable for our task, should be carefully selected to contain all possible solar wind and IMF contributions to the index. Otherwise rather small semiannual variability of solar wind driving would not be defined completely. In the previous investigations usually only general quality of a driving function was determined as a correlation coefficient between index and function. We used the alternative method, explicitly controlling selection of input parameters. The algorithm is easy to understand, considering the first example (Fig. 2). Details of the process and interpretation were described by Petrukovich (2006); Petrukovich and Rusanov (2005).

Figure 2a presents average a_p for logarithmically spaced bins of the driving function values (here, $E = VB_s$), taken for the same 3 hours, and separately for different V . It is evident, that solar wind speed contributes to the index more than just via VB_s . The equal vertical spacing between the curves at different E suggests an additive, rather than multiplicative modification, which will bring the curves closer. We select it as αV^2 , $\alpha = 7 \times 10^{-6} (\text{mV/m}) / (\text{km/s})^2$ (Fig. 2b) (also checked in the least squares sense). This procedure was repeated with the adjusted driving function and new tested solar wind parameters. The driving function always had the dimension of electric field and units of mV/m. Since the procedure is essentially iterative, initial choices are finally verified only in the end of the process. Therefore in Fig. 2b the final function with B_y dependence is used. IMF B_y input (not shown here) is optimized as $E = VB_z^* + \alpha V^2$, $B_z^* = \sqrt{B_y^2/2 + B_z^2} \sin^2(\theta/2)$. The

Table 1. Averaged a_p index and its solar wind model.

Parameter	Spring	Summer	Autumn	Winter
$\langle a_p \rangle$, nT	16.26	13.02	15.35	12.67
$\langle a_p \rangle$, nT (SW*)	15.91	12.52	14.70	11.92
$\langle a_p \rangle$, nT (E model)	15.93	12.53	14.72	11.93
$\langle a_p \rangle$, nT (E_2 model)	14.53	11.37	13.79	11.84

* only instants with available solar wind and IMF samples.

effect of solar wind density (Figs. 2c, d) is proportional to E and can be corrected with a multiplicative factor $(N/N_0)^{0.2}$. $N_0 = 7.18 \text{ cm}^{-3}$ is average density in our data set.

The effect of Mach numbers, solar wind ion temperature, β , IMF B_x , IMF variations was negligible. Finally,

$$E = 10^{-3} \cdot (N/7.18)^{0.2} (V \sqrt{B_y^2/2 + B_z^2} \sin^2(\theta/2) + 0.007 \cdot V^2) \quad (1)$$

Here magnetic field is in nT, solar wind speed is in km/s, density is in cm^{-3} , electric field – in mV/m. The correlation coefficient between E and a_p is 0.82 (for VB_s it is 0.56).

To verify robustness of our results we also constructed an alternative driving function E_2 fixing the velocity dependence to popular $\sim V^2$. Optimal dependencies on IMF B_y and density remained practically the same. 438.7 km/s is average speed in our data set.

$$E_2 = 10^{-3} \cdot (N/7.18)^{0.2} (V^2/438.7) \sqrt{B_y^2/2 + B_z^2} \sin^2(\theta/2) \quad (2)$$

The correlation coefficient between E_2 and a_p is 0.77.

We determine a_p driving functions separately for four seasons, centered on equinoxes and solstices (Fig. 3). Curves are approximated with linear interpolation/extrapolation. The number of points in the model was increased (cf. Figs. 2d and 3) to achieve necessary level of accuracy. Assuming $a_p = 1/N \sum_i P_i(E_i)$, difference in curves characterizes changes in magnetospheric response $P(E)$, while solar wind-related part of SAV is contained in seasonal sets of solar wind inputs E_i . Response functions for autumn and spring are similar. The winter response is lower as expected. The summer curve deviates from the winter one at higher inputs towards equinoctial responses (see also Sect. 4). Therefore we analyzed only the difference between winter and spring/autumn.

3 Semiannual index variation

Table 1 contains seasonal averages of a_p , which form the basis for our analysis. In what follows we discuss the results of the primary E model and return to E_2 model in the end of the section. For exact comparison we need to retain only the a_p subset with available solar wind measurements (Table 1,

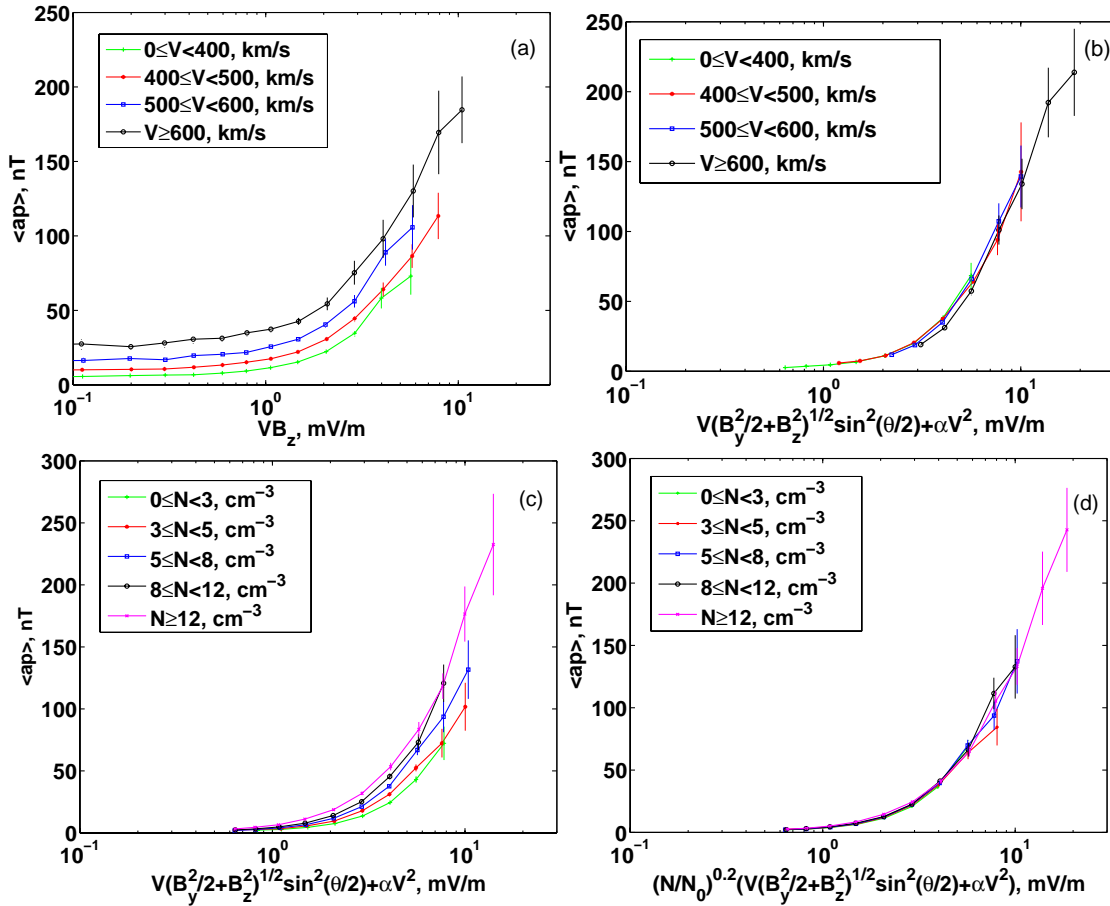


Fig. 2. Solar wind speed and density input to a_p . Thin vertical lines denote 90%-significance range of mean values. The averages from bins with less than 10 data points are not plotted.

line 2). Our model reproduces these values within about ~ 0.02 nT (Table 1, line 3). The 90% confidence range for a mean value estimate (of a Gaussian process, with a number of data samples $N \gg 1$) is $\sim 1.6 \times \sigma / \sqrt{N}$, where σ is the estimate of variance. In our cases this confidence range is 0.1–0.25 nT, depending on a season. An average of many unique $P_i(E_i)$, $i=1 \dots N$ can be equivalently described by a simple bilinear function of a histogram of solar wind inputs α_j , $\sum_j \alpha_j = 1$ (depending on a season) and responses at some predefined inputs E_j , $j=1 \dots K$:

$$a_p = \frac{1}{N} \sum_i P_i(E_i) = \sum_j \alpha_j P_j(E_j) = \alpha P \quad (3)$$

For simplicity in the following we drop summation signs. Relatively small variations of α and P from season to season can be introduced as $\Delta\alpha$ and ΔP . The difference between spring and winter is

$$\begin{aligned} a_{psp} - a_{pwi} &= (\alpha_{wi} + \Delta\alpha)(P_{wi} + \Delta P) - \alpha_{wi} P_{wi} \\ &= \alpha_{wi} \Delta P + \Delta\alpha P_{wi} + \Delta\alpha \Delta P. \end{aligned} \quad (4)$$

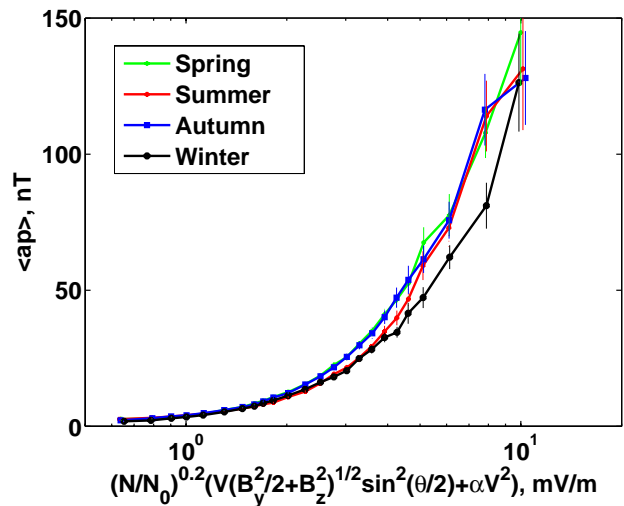


Fig. 3. a_p seasonal variations in driving function.

Table 2. Components of seasonal difference in nT.

Parameter	Total	Response	Solar wind	Nonlinear
spring-winter	4.00	2.29	1.32	0.38
autumn-winter	2.79	2.09	0.58	0.12

The first two members on the r.h.s. are, returning to the initial model:

$$\begin{aligned}\alpha_{wi} \Delta P &= \alpha_{wi} P_{sp} - \alpha_{wi} P_{wi} = P_{sp}(E_{wi}) - a p_{wi} \\ \Delta \alpha P_{wi} &= \alpha_{sp} P_{wi} - \alpha_{wi} P_{wi} = P_{wi}(E_{sp}) - a p_{wi}\end{aligned}\quad (5)$$

The first line is magnetospheric response contribution to SAV, the second one – solar wind contribution. The nonlinear term $\Delta \alpha \Delta P$ can be determined using the l.h.s. of Eq. (4) and results of Eq. (5). Results for the spring-winter and autumn-winter pairs are in Table 2.

In the frame of this approach the Russell-McPherron effect $\Delta a p^{RM}$ is a part of the solar wind contribution. We estimate its share in the first approximation as (M denotes GSM, Q denotes GSEQ frames):

$$a p = \alpha_M P_M = (\alpha_Q + \Delta \alpha) P_M = P_M(E_Q) + \Delta a p^{RM}\quad (6)$$

Contribution of the RM-effect in spring is 0.39 nT, in autumn – 0.36 nT, in winter – 0.13 nT.

Concluding with numbers, a_p SAV due to the magnetospheric response is rather stable $\sim 2\text{--}2.2$ nT (60–75%), while the solar wind related part of SAV is different in spring and autumn and is of the order of 20–30% (including <10% of Russell-McPherron effect). Nonlinear part is minor and less than 10%.

The E_2 model with the alternative form of solar wind speed input turned out to be substantially less accurate in reproducing seasonal averages of a_p (last line of Table 1). However, proportions between decomposed heliospheric and magnetospheric SAV sources were almost the same as in the primary model (not shown here).

4 Conclusions

Semiannual variation of geomagnetic activity is a bright observational phenomenon, and is a combination of several rather small sources. We investigate its composition in a_p index with a carefully selected quantitative model of solar wind driving. In this task we are interested only in statistical quality of this model, rather than in any physical interpretations.

Comparing with other suggested driving functions ($V B_s$ or $V^2 B$), we prefer the additive form ($V B_s + \alpha V^2$) of velocity dependence. Similar functional dependence is used in cross-polar cap potential drop modelling (e.g., Boyle et al., 1997). The general difference between additive and multiplicative corrections to a basic driving function is evident

comparing Figs. 2a and c. Proper choice of V -correction is most important for the northern-type IMF, when $V B_s$ is small (left side of Fig. 2a). Multiplication by one more V ($V^2 B_s$ -type function) results in a too small values and significant underestimation of the index (last line of Table 1). These small inputs occupy only a fraction of dynamic range and the problem can not be readily revealed during usual correlation analysis. Our results generally correspond to recent publications (see Introduction), relating more than half of semiannual variations to magnetosphere/ionosphere response and 20–30% to solar wind variability. Despite the clear difference between seasons statistical errors are not negligible. The RM effect and non-linear terms are at the margin of statistical significance. These numbers are relatively robust and can be reproduced qualitatively even with a not fully optimal driving function, here – of $V^2 B_s$ -type.

Since 11 of 13 a_p stations are located in the Northern Hemisphere, it is frequently argued, that a_p may contain an artificial periodicity related with seasonal asymmetry of hemispheres. In particular, the summer effect (Fig. 3) might be attributed to such north-south asymmetry. However, seasonal variability of alternative latitudinally equilibrated index am is also complex: winter averages of am , an , as are the same, but the summer values are different. Therefore the part of magnetospheric contribution might be due to inherent asymmetry between hemispheres or details of index derivation, which need to be taken into account in a further study. Also the average am and its variance are factor of 1.5 larger, than that of a_p , while the amplitude of SAV is the same. Therefore statistical problems are more significant for the am dataset.

Concluding, we suggest a formalized quantitative method to describe SAV in a_p index, which is consistent with previous results, provides error and nonlinearity estimates and a useful functional form for a further study of each source (magnetosphere and solar wind). However, further research will be more difficult, since smaller contributions are less definite statistically.

Acknowledgements. The work was supported by Russian grants HIII–5359.2006.2, MD-3036.2006.5, RFFI–07-02-00042.

Topical Editor I. A. Daglis thanks one anonymous referee for her/his help in evaluating this paper.

References

- Bohlin, J. D.: Extreme-ultraviolet observations of coronal holes, *Sol. Phys.*, 51, 377–398, 1977.
- Boyle, C. B., Reiff, P. H., and Hairston, M. R.: Empirical polar cap potentials, *J. Geophys. Res.*, 102, 111–125, 1997.
- Cliver, E. W., Kamide, Y., and Ling, A. G.: Mountains versus valleys: Semiannual variation of geomagnetic activity, *J. Geophys. Res.*, 105, 2413–2424, 2000.
- Cliver, E. W., Kamide, Y., and Ling, A. G.: The semiannual variation of geomagnetic activity: phases and profiles for 130 years of aa data, *J. Atmos. Sol.-Terr. Phys.*, 64, 47–53, 2002.

- Cliver, E. W., Svalgaard, L., and Ling, A. G.: Origins of the semi-annual variation of geomagnetic activity in 1954 and 1996, *Ann. Geophys.*, 22, 93–100., 2004.
- Cortie, A. L.: Sunspots and terrestrial magnetic phenomena, 1898–1911: The cause of the annual variation in magnetic disturbances, *Mon. Not. R. Astron. Soc.*, 73, 52–60, 1912.
- Finch, I. and Lockwood, M.: Solar wind-magnetosphere coupling functions on timescales of 1 day to 1 year, *Ann. Geophys.*, 25, 495–506, 2007, <http://www.ann-geophys.net/25/495/2007/>.
- Gonzalez, W. D., Joselyn, J. A., Kamide, Y., Kroehl, H. W., Rostoker, G., Tsurutani, B. T., and Vasyliunas, V. M.: What is a geomagnetic storm?, *J. Geophys. Res.*, 99, 5771–5792, 1994.
- Le Mouel, J.-L., Blanter, E., Chulliat, A., and Shnirman, M.: On the semiannual and annual variations of geomagnetic activity and components, *Ann. Geophys.*, 22, 3583–3588, 2004, <http://www.ann-geophys.net/22/3583/2004/>.
- Lyatsky, W., Newell, P. T., and Hamza, A.: Solar Illumination as Cause of the Equinoctial Preference for Geomagnetic Activity, *Geophys. Res. Lett.*, 28, 2353–2356, 2001.
- McIntosh, D. H.: On the annual variation of magnetic disturbance, *Philos. Trans. R. Soc. London. Ser. A.*, 251, 525–552, 1959.
- Petrukovich, A. A.: Solar wind density effect on the nightside geomagnetic activity (AL index), *J. Atmos. Sol.-Terr. Phys.*, 68, 1843–1849, 2006.
- Petrukovich, A. A. and Rusanov, A. A.: AL index dependence on the solar wind input revisited, *Adv. Space Res.*, 36, 2440–2444, 2005.
- Russell, C. T. and McPherron, R. L.: Semiannual Variation of Geomagnetic Activity, *J. Geophys. Res.*, 92–108, 1973.
- Svalgaard, L.: Geomagnetic Activity: Dependence on Solar Wind Parameters, in: *Coronal Holes and High Speed Wind Streams*, edited by: Zirker, J., Colorado Associated Universities Press, 371, 1977.
- Svalgaard, L., Cliver, E. W., and Ling, A. G.: The semiannual variation of great geomagnetic storms, *Geophys. Res. Lett.*, 29, 16, doi:10.1029/2001GL014145, 2002.